

SANDIA REPORT

SAND2004-2576
Unlimited Release
Printed June, 2004

Relaxation Nuclear Magnetic Resonance Imaging (R-NMRI) of Desiccation in M9787 Silicone Pads

Todd M. Alam, Brian R. Cherry and M. Kathleen Alam

Prepared by
Sandia National Laboratories
Albuquerque, New Mexico 87185 and Livermore, California 94550

Sandia is a multiprogram laboratory operated by Sandia Corporation,
a Lockheed Martin Company, for the United States Department of Energy's
National Nuclear Security Administration under Contract DE-AC04-94AL85000.

Approved for public release; further dissemination unlimited.



Issued by Sandia National Laboratories, operated for the United States Department of Energy by Sandia Corporation.

NOTICE: This report was prepared as an account of work sponsored by an agency of the United States Government. Neither the United States Government, nor any agency thereof, nor any of their employees, nor any of their contractors, subcontractors, or their employees, make any warranty, express or implied, or assume any legal liability or responsibility for the accuracy, completeness, or usefulness of any information, apparatus, product, or process disclosed, or represent that its use would not infringe privately owned rights. Reference herein to any specific commercial product, process, or service by trade name, trademark, manufacturer, or otherwise, does not necessarily constitute or imply its endorsement, recommendation, or favoring by the United States Government, any agency thereof, or any of their contractors or subcontractors. The views and opinions expressed herein do not necessarily state or reflect those of the United States Government, any agency thereof, or any of their contractors.

Printed in the United States of America. This report has been reproduced directly from the best available copy.

Available to DOE and DOE contractors from

U.S. Department of Energy
Office of Scientific and Technical Information
P.O. Box 62
Oak Ridge, TN 37831

Telephone: (865)576-8401
Facsimile: (865)576-5728
E-Mail: reports@adonis.osti.gov
Online ordering: <http://www.doe.gov/bridge>

Available to the public from

U.S. Department of Commerce
National Technical Information Service
5285 Port Royal Rd
Springfield, VA 22161

Telephone: (800)553-6847
Facsimile: (703)605-6900
E-Mail: orders@ntis.fedworld.gov
Online order: <http://www.ntis.gov/help/ordermethods.asp?loc=7-4-0#online>



SAND2004-2576
Unlimited Release
Printed June 2004

Relaxation Nuclear Magnetic Resonance Imaging (R-NMRI) of Desiccation in M9787 Silicone Pads

Todd M. Alam* and Brian R. Cherry
Department of Organic Materials

M. Kathleen Alam
Department of Chemical and Biological Sensing, Imaging and Analysis

Sandia National Laboratories
P.O. Box 5800
Albuquerque, NM 87185-0888

Abstract

The production and aging of silicone materials remains an important issue in the weapons stockpile due to their utilization in a wide variety of components and systems within the stockpile. Changes in the physical characteristics of silicone materials due to long term desiccation has been identified as one of the major aging effects observed in silicone pad components. Here we report relaxation nuclear magnetic resonance imaging (R-NMRI) spectroscopy characterization of the silica-filled and unfilled polydimethylsiloxane (PDMS) and polydiphenylsiloxane (PDPS) copolymer (M9787) silicone pads within desiccating environments. These studies were directed at providing additional details about the heterogeneity of the desiccation process. Uniform NMR spin-spin relaxation time (T_2) images were observed across the pad thickness indicating that the drying process is approximately uniform, and that the desiccation of the M9787 silicone pad is not a H_2O diffusion limited process. In a P_2O_5 desiccation environment, significant reduction of T_2 was observed for the silica-filled and unfilled M9787 silicone pad for desiccation up to 225 days. A very small reduction in T_2 was observed for the unfilled copolymer between 225 and 487 days. The increase in relative stiffness with desiccation was found to be higher for the unfilled copolymer. These R-NMRI results are correlated to local changes in the modulus of the material.

* Author to whom correspondence should be addressed: tmalam@sandia.gov

Acknowledgements

Sandia is a multiprogram laboratory operated by Sandia Corporation, a Lockheed Martin Company, for the United States Department of Energy's National Nuclear Security Administration under contract DE-AC04-94AL85000. This work is supported under the Sandia Research Foundation (RF) and the Enhanced Surveillance Campaign (ESC) program.

Contents

Abstract.....	3
Acknowledgements	4
Nomenclature	7
Introduction.....	8
Experimental Details	12
A. M9787 Silicone Pad.....	12
B. Desiccation	12
C. NMR Analysis.....	13
D. TG-IR Analysis.....	15
Results and Discussion.....	16
Conclusions.....	27
References.....	28

Figures

1. Spin echo decay and fit for the SiO₂ filled M9787 silicone pad.....18
2. 1D R-NMRI image of spin-spin relaxation (T₂) of M9787 silicone pads19
3. Histogram plot of the R-NMRI T₂ dispersal for the M9787 silicone pads.....20
4. Relative change in the stiffness versus desiccation time23
5. The percent weight loss for the M9787 silicone pads.....25

Tables

- I. Bulk NMR and R-NMRI ¹H spin-spin relaxation (T₂) results.17

Nomenclature

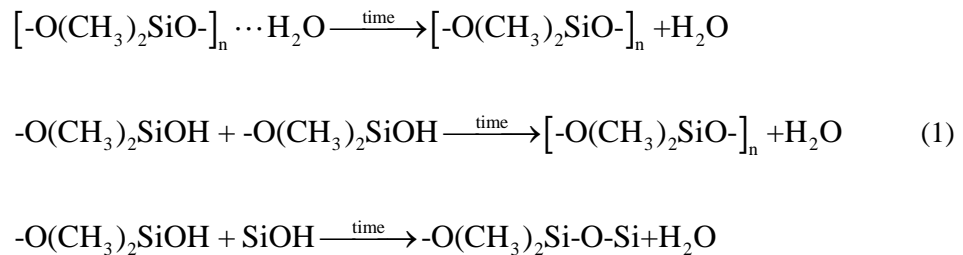
NMR	nuclear magnetic resonance
MRI	magnetic resonance imaging
R-NMRI	relaxation- nuclear magnetic resonance imaging
SPI	single point imaging
T ₂	spin-spin relaxation time
CPMG	Carr-Purcell-Meiboom-Gill
TG-IR	thermal gravimetric-infrared
DMS	dimethylsiloxane
DPS	diphenylsiloxane
MVS	methyl-vinylsiloxane
PDMS	polydimethylsiloxane
PDPS	polydiphenylsiloxane

Relaxation Nuclear Magnetic Resonance Imaging (R-NMRI) of Desiccation in M9787 Silicone Pads

Introduction

The role of aging in polysiloxane materials that are used in the weapon stockpile is still an area of active interest. The role of oxidation, hydrolysis, radiation and drying (desiccation) on the material performance has been investigated.¹⁻⁷ Desiccation of polysiloxane foams (for example the M97 series used in the W87) is now known to be an aging mechanism that leads to increased modulus (stiffening) of the pads within the pit assembly.^{1,4,8,9} In addition, the polysiloxane pads are one of the major water sources leading to corrosion on the actual pit. Understanding the source and the behavior of water in these materials is therefore important for the lifetime prediction of the siloxane materials.

The water within the siloxane materials can either result from the presence of physisorbed water (hydrogen bounds within the polymer matrix) or from chemisorbed water due to the migration and condensation of silanols (either from the polymer or from the silica filler) via^{10,11}



The loss of water from the polysiloxane material is often described by a thermally activated process that is given by

$$\frac{\partial[\text{H}_2\text{O}]}{\partial t} \approx \nu \exp(E_A / RT) f(\alpha) \quad (2)$$

where $f(\alpha)$ is a function that is determined by the rate limiting reaction mechanism.^{10,11}

In the M97 series silicones it has been *assumed* that for thin materials that the diffusion rate of water within the material was *not* the rate determining step. Previous studies have also assumed that water diffusion was not the limiting step for either the physisorbed or the chemisorbed waters described by Equation (1). On the other hand, long term desiccation effects on the order of years have been previously observed in silicone materials.¹²

The goal of the work describe in the SAND report was to specifically test the presence of diffusion-limited water transport leading to reduced chain mobility during the long-term desiccation. In particular we will concentrate of the silica-filled and unfilled M9787 silicone materials. Many of these materials are also been characterized using a variety of other techniques by collaborators at LLNL, KCP and Livermore-Sandia. Of particular interest was the use of the novel relaxation based nuclear magnetic resonance imaging (R-NMRI) techniques to provide images of the long term desiccation of the M9787 silicone pads.^{9,13}

Nuclear magnetic resonance (NMR) spectroscopy is a powerful tool in the monitoring of polymer aging and the elucidation of aging mechanisms at the molecular level. A wide variety of studies using ¹H, ¹³C, and ¹⁷O NMR spectroscopy have been

utilized to investigate degradation mechanisms in thermally and oxidatively-aged polymers (see references [5,14] and citations within). Polymer chain mobility and segmental motion is a characteristic that can be related to material properties. NMR spectroscopy probes these polymer motions through measurement of nucleus spin-relaxation data. The spin-spin relaxation time (T_2) is one parameter that has been used to characterize the aging effects on various polymer materials.^{14,15} Reduction of the T_2 relaxation time with aging signifies a reduction in the polymer chain mobility, such as would be observed during chain cross-linking.^{3,16-19}

Magnetic resonance imaging (MRI) is a nondestructive means of generating spatial pictures of a wide variety of materials.²⁰⁻²² MRI utilizes magnetic field gradients to impart a spatially dependent resonance frequency on the nuclei probed. Thereby images dependent on the location of nuclei (most commonly ^1H) are generated. MRI techniques have been developed to handle the broad resonance lines and short T_2 associated with solids, facilitating the study of a variety of materials from polymers to ceramics.^{14,23-36} Single point imaging (SPI), also known as constant time imaging, developed by Emid and Creyghton,³⁷ is ideally suited to study materials with very short T_2 relaxation times.

The advantages of NMR spectroscopy and MRI techniques can be coupled to provide valuable insights into the mechanisms and processes of aging. Relaxation nuclear magnetic resonance imaging (R-NMRI) generates an image with various NMR relaxation times measured for each voxel.^{8,14,23,31-35,38-41} A voxel is the smallest volume element measured during the experiment. The R-NMRI experiments implemented in this study

measure the ^1H spin-spin relaxation times (T_2) for each voxel of the image. The T_2 measurements were carried out using a spin echo approach.

To demonstrate the applicability of R-NMRI, the effect of desiccation on the NMR T_2 relaxation (and corresponding chain mobility) for the M9787 silicone pad is presented. Continued desiccation causes a decrease in the average or bulk T_2 values over a period of years, indicating the removal of water produces a stiffening of the siloxane material.^{1,11,42,43} In this R-NMRI imaging study the possible presence of diffusion-limited processes leading to heterogeneous aging are explored.

Experimental Details

A. M9787 silicones

The silica-filled and unfilled M9787 silicones were obtained from Honeywell/FM&T (Kansas City, MO) and used without further preparation. The copolymers are comprised of approximately 90.6 wt. % dimethyl-siloxane (DMS), 9.0 wt. % diphenyl-siloxane (DPS), and 0.4 wt. % methyl-vinyl-siloxane (MVS). The silica filled copolymer was prepared by milling a mixture of 21.6 wt.% fumed silica (Cab-o-Sil M7D, Cabot, Tuscola, IL), 4.0 wt.% precipitated silica (HiSil 233, PPG Industries, Pittsburgh, PA), 6.8 wt.% ethoxy-endsblocked siloxane processing aid (Y1587, Union Carbide, Danbury, CT) with the copolymer. After bin aging for 3 weeks at room temperature, both the filled and unfilled siloxane gums were cross-linked with a thermally activated peroxide-curing agent. Typical sample thickness was 2.5 mm.

B. Desiccation

The siloxane copolymer samples were placed in a desiccator containing P_4O_{10} and allowed to dry. At different desiccation times, a portion of the polymer sample (2mm x 2mm x 2.5mm) was cut from the center of the pad so that desiccation occurred primarily in one dimension. The cut sample was placed in a standard NMR tube with the desiccation-exposed surface aligned perpendicular to the applied imaging gradient field, and analyzed at room temperature.

C. NMR Analysis

The ^1H R-NMRI spectra were collected on a Bruker DRX400 spectrometer using a standard 5 mm broadband probe with a single axis gradient operating at a resonant frequency of 399.9 MHz. To handle the short T_2 of solid materials Single Point Imaging (SPI),^{34,35,37,39-41} or Constant Time Imaging techniques were implemented. A maximum gradient strength of 40 Gauss cm^{-1} , 8 scan averages, a 345 μs phase encoding time, 48 gradient steps, and a 4 mm field of view resulting in a calculated resolution of 83 μm along the imaging gradient. A repetition time of 4 s was used to avoid saturation effects and ensure a safe duty cycle for the NMR probe. A traditional spin echo filter with 31 different echo delays times was placed prior to the SPI sequence to allow measurement of T_2 relaxation times for each voxel. A z -storage period of 37 μs was utilized after the spin echo and prior to the SPI sequence as previously described.²³ During the z -storage period, the gradients were switched on and allowed to stabilize, reducing the effects of eddy currents. Phase cycling of the z -storage placed the magnetization along the $\pm z$ -axis to eliminate the effects of T_1 relaxation during the storage period.²³ Bulk T_2 measurements were collected with the traditional spin echo pulse sequence utilizing an 8.5 μs ($\pi/2$) pulse, 4 scans, one dummy scan, and a 1 s recycle delay. The same 31 echo delay periods implemented in the R-NMRI were used for the bulk relaxation experiments. The use of a spin echo based method for T_2 measurement was implemented instead of a Carr-Purcell-Meiboom-Gill (CPMG)^{44,45} echo train in order to allow the measurement of very short T_2 that could potentially be present in a rigid solid. In addition, the accuracy in fitting the multi-exponential T_2 decay of the PDMS copolymers (see below) was improved through

the use of the spin echo filter.²³ The one-dimensional (1D) R-NMRI images reported in this study represent a projection of a slice along a single axis, essentially providing an average over a 83 μm x 2.0 mm x 2.0 mm slice.

The motional processes in multi-component siloxanes are complex,^{1-3,16-19,25} such that the segmental motion may not be defined by a single correlation time. It is well known that the signal intensity, $I(\tau)$, during the spin echo decay for PDMS is best described by a double exponential decay^{2,16-19}:

$$I(\tau) = X_A \exp(-2\tau/T_{2A}) + (1 - X_A) \exp(-2\tau/T_{2B}). \quad (3)$$

where τ is the echo spacing, X_A and $(1 - X_A)$ define the relative fraction of component A and B , and T_{2A} and T_{2B} define the T_2 relaxation time for component A and B , respectively. The cross-linked or entangled network species, with the respectively short T_{2A} relaxation comprises a majority of the material. The species with the long T_{2B} spin-spin relaxation time have been assigned to the low molecular weight species separated from the network and dangling chain ends of the network that have a higher mobility.^{2,16-19} At short τ , the echo decay has mixed Gaussian-exponential behavior indicative of inhomogeneous averaging of the dipolar couplings.² The very first part of the decay (which is Gaussian) was ignored during our analysis with the spin echo intensity being fit to the double exponential defined in Eqn. (3) (Figure 1).

D. TG-IR Analysis

Thermal-gravimetric (TG) data was collected using a Netzch STA-449 system. Approximately 30 milligrams of each sample was used. The samples were placed in an Al₂O₃ sample cup and allowed to equilibrate with the dry, N₂ flow gas (approximately 10 minutes), with N₂ flow rates were maintained at 100 cc total (60/40 split between balance purge and sample purge). Temperature ramps were started at ambient temperature (~25 °C) and increased at 10 °C/min until 500 °C was reached. The flow from the TG was directed, via a heated transfer line (190 °C), to a Bruker Equinox FTIR equipped with a heated 10 cm gas cell (180 °C). Infrared data was collected during the entire TG ramp, at a rate of approximately one averaged sample every 14 seconds. Data were collected at 2 cm⁻¹ resolution across the range 4000-700 cm⁻¹ using an MCT detector.

Results and Discussion

A ^1H NMR spectrum of the M9787 silicone pad is comprised of two asymmetric resonances at $\delta = 0$ and $+7$ ppm, assigned to the methyl and phenyl protons respectively. Table 1 lists the T_2 relaxation data obtained for the filled and unfilled pads. For each desiccation time, the bulk T_2 relaxation was determined as described by Eqn. (3) for the individually integrated methyl and phenyl protons, and for the total integrated spectral intensity (Figure 1). In agreement with the previous ^1H studies of these materials,^{2,16-19} the relaxation data is dominated by the cross-linked network species as evident by the large X_A fraction (> 0.92). In the unfilled material, the short relaxation time component fraction (X_A) increases with desiccation, reflecting an increase in cross-linking and/or formation of entanglements that reduce chain mobility. In the SiO_2 -filled pad there is not a significant increase in the fraction of the immobile or short relaxation time component.

Table 1. The ^1H spin-spin relaxation (T_2) determined from bulk NMR measurements and the R-NMRI experiment for the SiO_2 -filled and unfilled M9787 silicone pad as a function of desiccation time.

Time	PDMS/ PDPS	Bulk T_2 [ms]									T_2 R-NMRI (mean) [ms] ^b
		T_{2A} ^a			T_{2B} ^a			X_A			
		Total	Methyl	Phenyl	Total	Methyl	Phenyl	Total	Methyl	Phenyl	
0	SiO_2 - filled	1.90	1.83	2.94	15	15	13	0.95	0.95	0.95	1.92 ± 0.01
	Unfilled	2.16	2.08	3.22	16	16	19	0.92	0.92	0.90	2.02 ± 0.01
225 days	SiO_2 - filled	1.71	1.64	2.60	19	20	8	0.96	0.96	0.93	1.65 ± 0.01
	Unfilled	1.40	1.33	2.17	29	30	20	0.96	0.96	0.94	1.30 ± 0.01
487 days	SiO_2 - filled	1.65	1.58	2.43	13	13	15	0.96	0.95	0.94	1.67 ± 0.01
	Unfilled	1.41	1.33	2.26	31	32	28	0.96	0.96	0.95	1.22 ± 0.01

^a Error ($T_{2A} \pm 0.05$ ms; $T_{2B} \pm 1$ ms) determined from the uncertainty in linear regression. The large error in T_{2B} is primarily due to the small fraction of this component in the copolymer.

^b Error in images, $\sigma(T_2)$, determined from the uncertainty in linear regression ($T_2 \pm 0.05$ ms). For 30 T_2 measurements present in each R-NMRI image, the standard deviation of the mean is given by $\sigma(T_2)/\sqrt{30}$.

The 1D R-NMRI images based on T_2 relaxation for the SiO_2 -filled and unfilled M9787 silicone pads are shown in Figure 2a and 2b, respectively. The spatial dimension of the relaxation images are perpendicular to the surface directly exposed to the dry desiccation environment, such that the left and right sides of Figure 2 correlates to the upper/lower sample surfaces in contact with the desiccating atmosphere. The changes in T_2 with desiccation are further illustrated in Figure 3, which shows histogram distribution of the T_2 values as a function of desiccation time. There is a reduction of the overall T_2 value with desiccation for both the SiO_2 -filled and unfilled M9787 silicone pads through 225 days, with the unfilled material showing the largest change. For the unfilled material, there is a small but continued reduction in the measured T_2 value even after 487 days. It

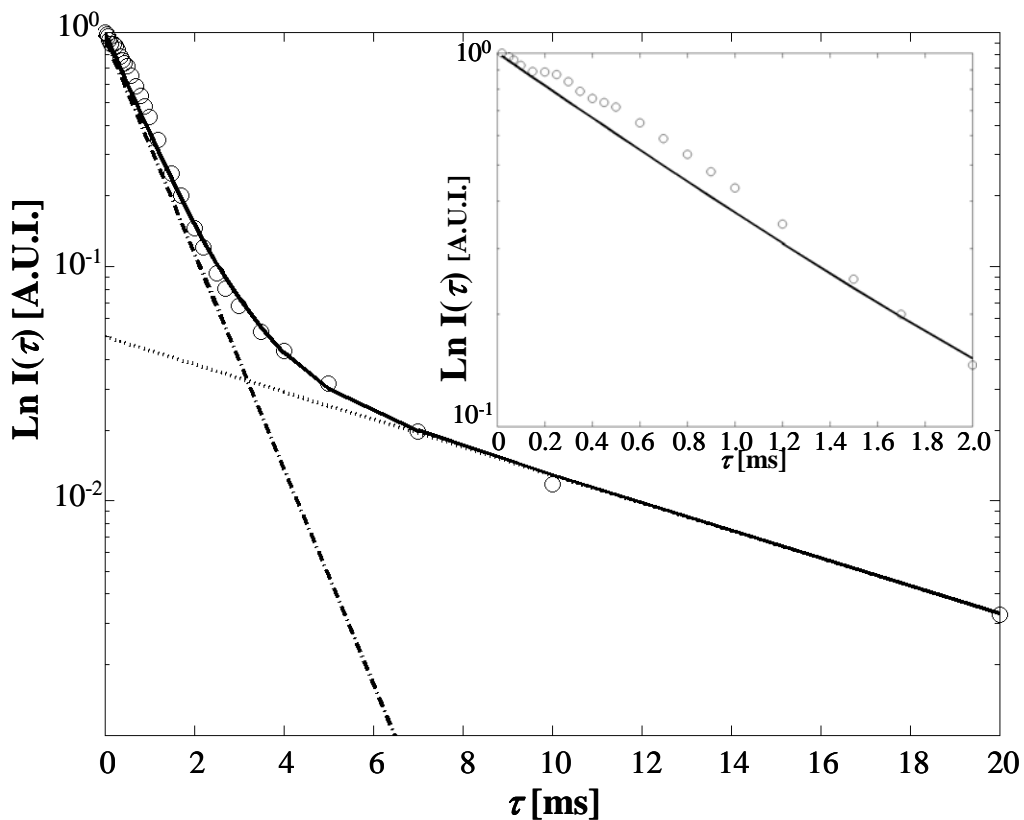


Figure 1: Representative double exponential fit of the signal intensity $I(\tau)$ from spin-echo decay experiments of the silica-filled M9787 silicone pad prior to desiccation. The open circles are the spin echo intensity for the total ^1H signal, the solid black line is the fit based on Equation 1, the gray dashed-dotted line is the curve for a single exponential decay with constant T_{2A} , and the dotted line is for a single exponential decay with constant T_{2B} . The inset is the short echo time region expanded to show the small Gaussian behavior.

should be noted that from previous studies, changes in T_2 have been noted for desiccated samples beyond 2 years.⁴⁶

A comparison of the mean T_2 measured in the R-NMRI experiments and the bulk T_{2A} values (Table 1), indicates that the mean T_2 measured by the imaging experiment are the same as those determined from bulk measurements. Accurate determination of the small fraction (X_B) component with the long T_{2B} values (the low molecular weight and dangling chain ends) during imaging was not possible due to the low signal to noise ratios at long

spin echo times of the R-NMRI data. The similar T_2 values, in the filled and unfilled M9787 silicone pads before desiccation, shows that the chain and segmental dynamics are similar in these materials. The reduction in T_2 (both bulk and imaging) corresponds to a decrease in the local chain mobility.^{3,4,47,48} The magnitude of T_2 has been shown to be inversely proportional to the reduced effective dipolar coupling, $T_2^{-1} \approx \langle \Omega_d^2 \rangle$.^{4,47,48} With reduced chain and segmental motions, the averaging of the ^1H - ^1H dipolar coupling becomes less, leading to an increase in $\langle \Omega_d^2 \rangle$. In the SiO_2 -filled M9787 silicone pad, the effects of desiccation on the observed T_2 values are smaller than the unfilled and become negligible after 225 days, demonstrating that the presence of SiO_2 helps minimize the effects of drying.

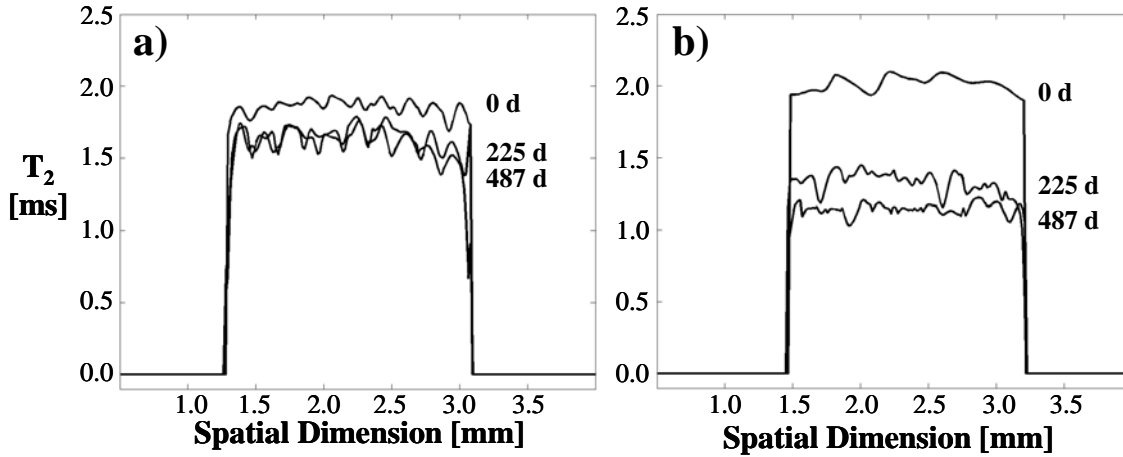


Figure 2: One-dimensional R-NMRI image of spin-spin relaxation (T_2) measured across the M9787 silicone pad for: **a)** SiO_2 -filled, **b)** unfilled materials. The number of days the samples were exposed to desiccation is shown next to each image (0, 225, and 487 days, respectively).

Based on the rapid diffusion of water in silicones it has been argued that desiccation should not be a diffusion-limited process. Using the reported diffusion coefficients for PDMS ($1.6\text{--}1.8 \times 10^{-9} \text{ m}^2\text{s}^{-1}$) only 7 to 9 minutes would be required for

H₂O to diffuse across the 2.5 mm sample thickness.^{49,50} However, the observation of desiccation effects proceeding on the timescale of years argues against a simple diffusive process, and initially prompted these imaging studies. In addition, images obtained

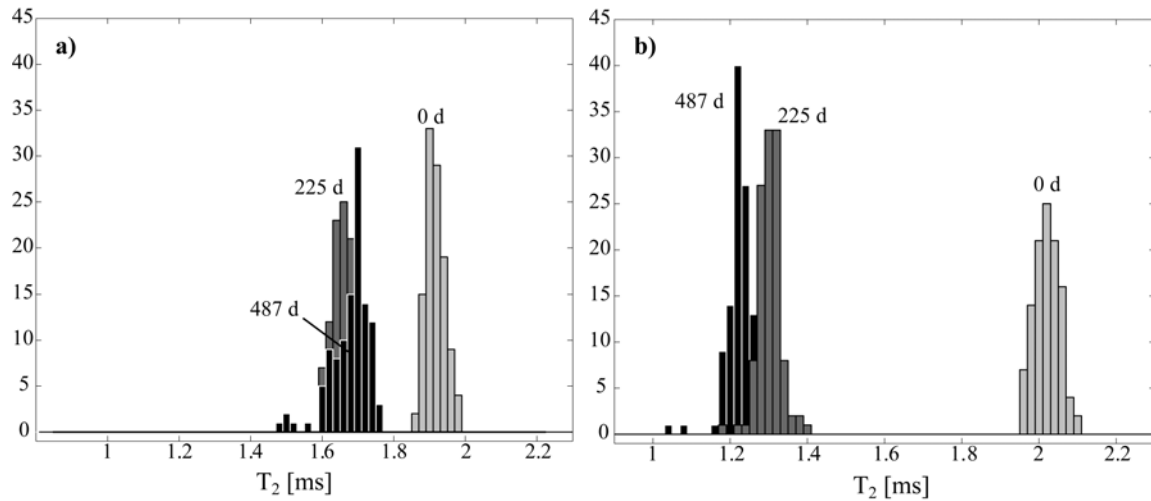


Figure 3: Histogram plot of the R-NMRI T₂ dispersal a) SiO₂-filled M9787 silicone pad, b) unfilled M9787 silicone pad. The light gray curve (0 d) is for the sample prior to desiccation, the dark gray curve (225 d) was taken after 225 days of desiccation, and the black curve (487 d) is after 487 days of desiccation. Each bin is 20 μs wide.

following 6 days of desiccation are identical to the un-desiccated material, revealing that T₂ variations occur on a longer time scale. For both materials, a rather uniform T₂ profile was observed spatially across the sample for each desiccation time. Because the R-NMRI image is a simple one-dimensional picture of the material, the T₂ measured for each voxel is an average value for each 2D plane perpendicular to the imaging axis (magnetic field), and parallel to the exposed surface. The uniform T₂ profiles imply that the diffusion rate of water is rapid enough that water is transported from the polymer in a uniform manner,

without the formation of a chain dynamic gradient within the material, and that the rate of H₂O loss from the polymer is significantly slower than the H₂O diffusion rate within the polymer.

The H₂O within the M9787 silicone pad is known to arise from several sources (Eqn 1): a) residual or adsorbed water present in the siloxane following production and processing, b) water produced from the internal condensation of Si-OH present within the siloxane, and c) water present on the silica-filler surface. Dihn *et al.* have shown that the majority of the 1 % wt. loss occurring in silica-filled siloxanes upon desiccation is from the water and Si-OH on the silica filler surface.¹¹ The loss of interfacial water has been shown to increase the long-range hydrogen bonding interactions between the Si-OH on the silica filler surface and the oxygen of the polymer backbone.^{1,42,43,48} Additionally, water lost at the silica surface or from the polymer species will give rise to increased entanglement of the polymer chains, thereby reducing chain mobility (consistent with a reduction in T₂). Similarly, physical cross-links formed during the internal condensation of SiOH groups also give rise to reduced chain mobility, and corresponding reduction of the observed T₂ parameters.

In many instances, material performance depends on the heterogeneity of this degradation/aging process at the micron scale. Experimental measurement of this heterogeneity could benefit computational modeling of the aging process. While the 1D R-NMR images in Figure 2 did not reveal classic diffusion limited heterogeneity, more information about the potential heterogeneities in the copolymers may lie in the observed width of the T₂ distribution (Figure 3). Previous MRI studies of polymeric materials have shown a variation in the T₂ distribution width with aging or swelling, where the width is a

measure of heterogeneity.³¹⁻³³ Recall, the R-NMRI T_2 images in Figure 2 are not revealing differences in ^1H density, but instead are showing the local relaxation parameters of the ^1H density in that image slice. The distribution of T_2 obtained for both the filled and unfilled materials (Figure 3) shows a very small increased distribution width with desiccation time (compare 0 days to 487 days), but these changes are on the same order as experimental error. Therefore, no definitive variation in the T_2 distribution widths (corresponding to heterogeneities in chain dynamics) was observed in the R-NMRI of these materials.

The question of whether the smaller variations in the T_2 times at longer desiccation times represent real changes in the materials, reveal heterogeneities, or are within experimental error also needs to be discussed. In Table 1, it can be seen that the values for the bulk T_2 and mean R-NMRI T_2 measurements, as well as trends are slightly different. From an experimental point of view, the bulk T_2 measurements are expected to be more precise due to large sample volume detected, higher signal to noise, and a less complicated pulse sequence. On the other hand, the bulk T_2 measurement is an average T_2 value over the entire sample volume (2 mm x 2 mm x 2.5 mm), while the R-NMRI is the average of 30 separate T_2 measurements (2 mm x 2 mm x 83 μm). It has been suggested that the differences between the bulk and the average R-NMRI data, as well as the differences between the 256 and 487 day data of the copolymers may be due to heterogeneities in the polymer, or experimental error. The T_2 distribution from the 30 different R-NMRI slices (Figure 3) gives a measure of the error and any heterogeneity over a 2.5 mm length scale. Larger heterogeneities (> 10 mm) are not expected to be

present within these materials. These distributions (Figure 3a) clearly show that there are no significant differences between the 225 and 487 day T_2 values in the SiO_2 -filled

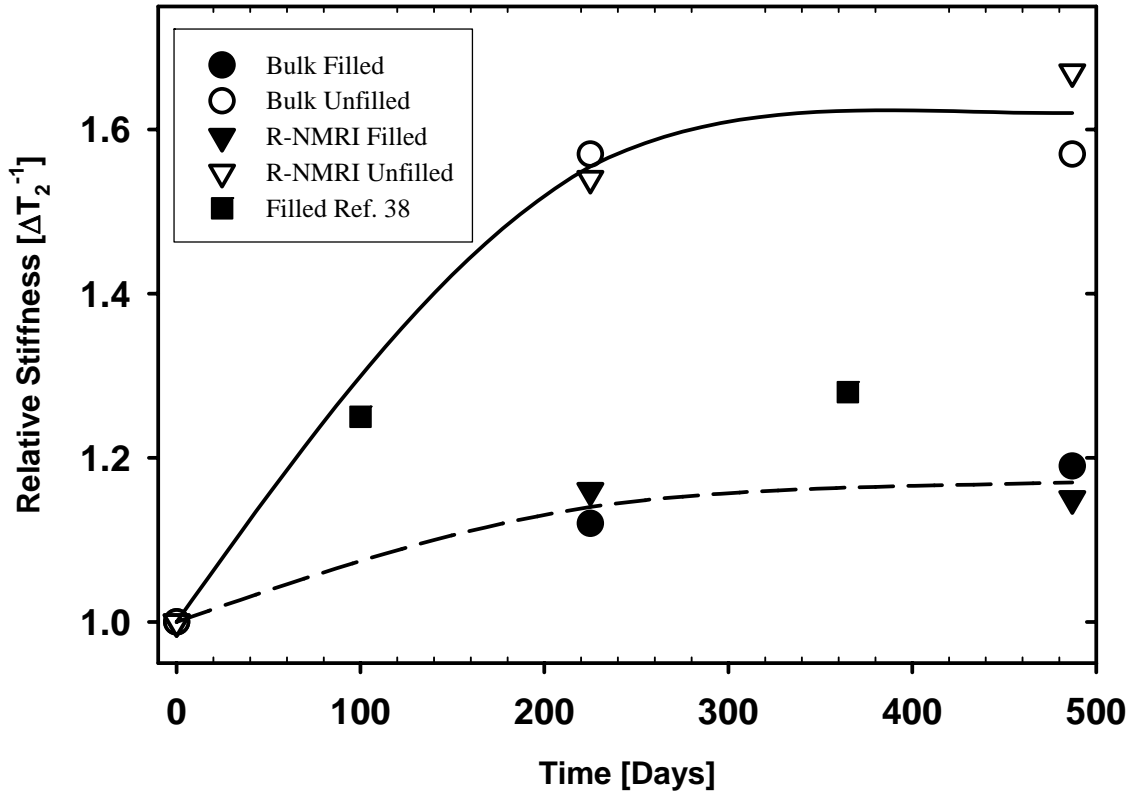


Figure 4: Relative change in the stiffness, $\Delta(T_2^{-1})$, of the copolymers with desiccation as measured by the relative change in the inverse spin-spin relaxation (T_2^{-1}), see Equation 2. The filled symbols depict the $\Delta(T_2^{-1})$ values for the silica filled copolymers while the open symbols are for the unfilled M9787 silicone pad. The circles represent the bulk T_2 measurements and the triangles are for the mean R-NMRI measured T_2 values. The filled squares are the relative stiffness measured for similar silica-filled copolymers and are shown for comparison.¹ Lines are meant as guides for the eye.

material (within experimental data). In contrast, the distributions in Figure 3b, reveal that for the unfilled material there is a small distinct change between 225 and 487 days of desiccation. This type of distribution analysis reveals the weakness of relying on a single

T_2 value (bulk or average) to address small T_2 changes occurring within the material. The estimated error given in Table 1 for the mean R-NMRI T_2 values was determined from the standard deviation of mean (SDOM) for the 30 measured T_2 values for each T_2 -map (Figure 2).

A further comparison between the filled and unfilled PDMS/PDPS copolymers is shown in Figure 4. The relative stiffness, defined as:

$$\Delta(T_2^{-1}) = \frac{T_2(t)^{-1}}{T_2(0)^{-1}} \quad (4)$$

for the two materials is plotted as a function of desiccation time (t). The relative stiffness, measured by Maxwell *et al.*^{1,48} for a SiO₂-filled PDMS/PDPS copolymer, is plotted for comparison and is consistent with the present results. The increased effect on the relative stiffness during desiccation of the unfilled copolymer is apparent. In previous studies of desiccation effects on PDMS/PDPS copolymers, Maxwell and co-workers concluded that the increased stiffness in silica filled copolymer is a result of water removal from the surface of the silica filler. When this water was removed, the interaction strength (hydrogen bonding) between the silica filler and the polymer chain increases causing the segmental motion of the polymer chains to be reduced.^{1,42,43,48} For the unfilled siloxane material, this interaction with the SiO₂ filler is not a possibility and requires an additional explanation to explain the large increase in relative stiffness upon desiccation (Figure 4).

It has been argued that the difference in the relative stiffness between the unfilled and filled siloxane copolymers is due to non-equivalent water content in the samples,

with SiO₂-filled copolymers containing more water. Dihn *et al.* utilized a mass spectroscopy detected temperature-programmed desorption technique to quantify the

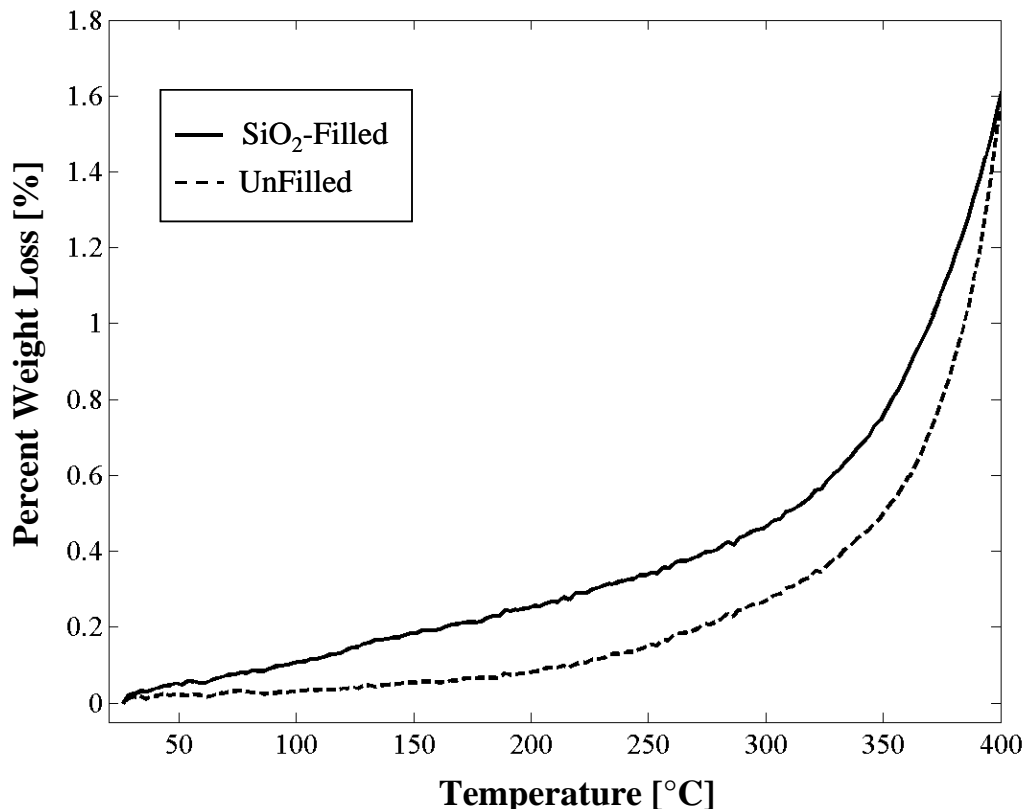


Figure 5: The percent weight loss for the SiO₂-filled (solid line) and unfilled (dashed line) M9787 silicone pad, respectively as a function of temperature determined from TG-IR. At low temperatures (below 350°C), H₂O is the dominant volatile species in the SiO₂-filled material, in the unfilled material organic alkanes are also out-gassed.

water content and concluded that the additional water present in the filled materials is present on the SiO₂ filler surface.¹¹ To address this question for the present siloxane materials thermal-gravimetric Infrared (TG-IR) data for the M9787 silicone pads were obtained. The weight loss as a function of temperature is shown in Figure 5. These TG-IR results show that the SiO₂-filled materials indeed contain more water (0.2 to 0.4 wt %) than the unfilled siloxanes, even though a portion of the weight loss in the unfilled

copolymer was due to volatilization of alkanes. The TG-IR data also reveals that decomposition of the M9787 silicone pad occurs at temperatures above 350°C, at which point the siloxanes volatilized. Even though there is a difference in the total water content in the SiO₂-filled and unfilled pads, the similarity in T₂ values prior to desiccation shows that the chain dynamics are similar, and do not correlate with the overall water content.

The changes in T₂ (relative stiffness) may be related to the different water loss during desiccation, with decreased change in relative stiffness for the SiO₂-filled material resulting from the silica filler reducing or hindering the production of new entanglements and/or cross-links of the polymer chains, or that the rate of water loss from SiO₂-filled materials is reduced. Water sorption of silica-filled PDMS is a factor of five higher than the unfilled material,⁵⁰ suggesting a stronger affinity of water at the SiO₂-siloxane surface. For the unfilled M9787 silicone pad the larger observed changes in relative stiffness suggest that desiccation favors the production of entanglements and/or cross-links within this material.

A final question, how do these variations in T₂ relate to changes in the physical properties of the material? In similar PDMS/PDPS copolymers, T₂ has been related to the equilibrium storage modulus (G')^{3,18}:

$$\frac{1}{T_2} \approx C G'^2 \quad (5)$$

where C is proportionality constant (material dependant). More recent reports have presented a linear relationship.^{1,4} The proportionality constant C has not been explicitly determined for the copolymer studied; however, the general relationship between T₂ and

the storage modulus is expected to hold. Based on the data reported by Maxwell *et al.*,³ C was found to be approximately $21 \text{ MPa}^{-2}\text{s}^{-1}$ for a RTV-5370 PDMS/PDPS copolymer. If we assume a similar proportionality constant for the M9787 silicone pad, the estimated total change in equilibrium storage modulus ($\Delta G'$) with desiccation is 8% and 29% for the filled and unfilled materials respectively. These types of relationships allow the effective imaging of physical properties such as modulus to be carried out.

Conclusion

Relaxation nuclear magnetic resonance imaging (R-NMRI) provided insights into the desiccation process occurring within M9787 silicone pads. Reduction of the spin-spin relaxation times (T_2) with desiccation is uniform ($\sim 100 \mu\text{m}$ scale) across the sample thickness, indicating the hardening of the M9787 silicone pad is not H_2O diffusion limited within the material. The silica filled material appeared to be stabilized from further desiccation effects past 225 days while a continued small reduction in T_2 was observed for the unfilled copolymer through 487 days of desiccation. The relative stiffness for both the filled and unfilled M9787 silicone pads increased with desiccation, consistent with previous studies.^{1,48} However, the relative stiffness of the unfilled materials was more strongly affected. The affinity of water to the SiO_2 -siloxane interface is proposed as the reason for the differences between the desiccation behavior in the SiO_2 -filled and unfilled M9787 silicone pads.

References

- (1) Maxwell, R. S.; Balazs, B.; Cohenour, R.; Prevedel, E. *Macromolecular Symposia* **2003**, *202*, 291.
- (2) Maxwell, R. S.; Balazs, B. *J. Chem. Phys.* **2002**, *116*, 10492.
- (3) Maxwell, R. S.; Cohenour, R.; Sung, W.; Solyom, D.; Patel, M. *Polymer Degrad. Stabil.* **2003**, *80*, 443.
- (4) Maxwell, R. S.; Balazs, B. *Nucl. Instr. Meth. Phys. Res. B* **2003**, *208*, 199.
- (5) Alam, T. M.; Celina, M.; Assink, R. A.; Clough, R. L.; Gillen, K. T.; Wheeler, D. *R. Macromolecules* **2000**, *33*, 1181.
- (6) Solyom, D.; Cohenour, R. E.; Eastwood, E. A.; Nail, E. A.; Sung, B. *Proceedings of the 25th Aging, Compatibility, and Stockpile Stewardship Conference* **2003**, 29.
- (7) Chinn, S. C.; Balaz, B.; Maxwell, R. S. *Proceedings of the 25th Aging, Compatibility, and Stockpile Stewardship Conference* **2003**, 319.
- (8) Mayele, M.; Oellrich, L. R. *Appl. Spec.* **2004**, *58*, 338.
- (9) Cherry, B. R.; Alam, T. M. *Proceedings of the 25th Aging, Compatibility, and Stockpile Stewardship Conference* **2003**, Livermore, CA, Nov. 18.
- (10) Dihn, L. N.; Schildbach, M. A.; Maxwell, R. S.; Siekhaus, W. J.; Balaz, B.; McLean II, W. *Proceedings of the 25th Aging, Compatibility, and Stockpile Stewardship Conference* **2003**, 43.
- (11) Dihn, L. N.; Balooch, M.; LeMay, J. D. *J. Colloid Inter. Sci.* **2000**, *230*, 432.
- (12) Maxwell, R. S. *Personal Communication* **2004**.
- (13) Cherry, B. R.; Alam, T. M. *Polymer* **2004**, *In Press*.
- (14) Garbarczyk, M.; Kuhn, W.; Klinowski, J.; Jurga, S. *Polymer* **2002**, *43*, 3169.

- (15) Assink, R. A.; Celina, M.; Gillen, K. T. *Polymer News* **2003**, 28, 102.
- (16) Folland, R.; Charlesby, A. *Radiat. Phys. Chem.* **1976**, 8, 555.
- (17) Folland, R.; Charlesby, A. *Radiat. Phys. Chem.* **1977**, 10, 493.
- (18) Chien, A.; Maxwell, R. S.; Chambers, D.; Balazs, B.; LeMay, J. *Rad. Phys. Chem.* **2000**, 59, 493.
- (19) Charlesby, A.; Folland, R. *Radiat. Phys. Chem.* **1983**, 15, 393.
- (20) Lauterbur, P. *Nature* **1973**, 242, 190.
- (21) Kumar, A.; Welti, D.; Ernst, R. R. *J. Mag. Res.* **1975**, 18, 69.
- (22) Kumar, A.; Welti, D.; Ernst, R. R. *Naturwissenschaften* **1975**, 62, 34.
- (23) Beyea, S. D.; Balcom, B. J.; Prado, P. J.; Cross, A. R.; Kennedy, C. B.; Armstrong, R. L.; Bremner, T. W. *J. Mag. Res.* **1998**, 135, 156.
- (24) Barth, P.; Hafner, S.; Denner, P. *Macromolecules* **1996**, 29, 1655.
- (25) Garrido, L.; Mark, J. E.; Sun, C. C.; Ackerman, J. L.; Chang, C. *Macromolecules* **1991**, 24, 4067.
- (26) Blümli, P.; Blümich, B. *Macromolecules* **1991**, 24, 2183.
- (27) Prado, P. J.; Gasper, L.; Fink, G.; Blümich, B. *Appl. Magn. Reson.* **2000**, 18, 177.
- (28) Fang, Z.; Hoepfel, D.; Winter, K. *Mag. Res. Imag.* **2001**, 19, 501.
- (29) Beyea, S. D.; Balcom, B. J.; Bremner, T. W.; Prado, P. J.; Cross, A. R.; Armstrong, R. L.; Grattan-Bellow, P. E. *Solid State Nuc. Mag. Res.* **1998**, 13, 93.
- (30) Beyea, S. D.; Balcom, B. J.; Mastikhin, I. V.; Bremner, T. W.; Armstrong, R. L.; Grattan-Bellow, P. E. *J. Mag. Res.* **2000**, 144, 255.
- (31) Barth, P.; Hafner, S. *Mag. Res. Imag.* **1997**, 15, 107.
- (32) Malveau, C.; Grandclaude, D.; Canet, D. *J. Mag. Res.* **2001**, 150, 214.

- (33) Chaumette, H.; Grandclaude, D.; Canet, D. *J. Mag. Res.* **2003**, *163*, 369.
- (34) Blümich, B. *Concepts in Mag. Res.* **1999**, *11*, 147.
- (35) Balcom, B. J.; MacGregor, R. P.; Beyea, S. D.; Green, D. P.; Armstrong, R. L.; Bremner, T. W. *J. Mag. Res. A* **1996**, *123*, 131.
- (36) Szomolanyi, P.; Goodyear, D.; Balcom, B. J.; Matheson, D. *Mag. Res. Imag.* **2001**, *19*, 423.
- (37) Emid, S.; Creighton, J. H. N. *Physica* **1985**, *128B*, 81.
- (38) Gussoni, M.; Greco, F.; Mapelli, M.; Vezzoli, A.; Ranucci, E.; Ferruti, P.; Zetta, L. *Macromolecules* **2002**, *35*, 1722.
- (39) Balcom, B. J.; Bogdan, M.; Armstrong, R. L. *J. Mag. Res. A* **1996**, *118*, 122.
- (40) Chudek, J. A.; Hunter, G. *Annual Reports on NMR Spec.* **2002**, *45*, 151.
- (41) Ghosh, P.; Laidlaw, D. H.; Fleischer, K. W.; Barr, A. H.; Jacobs, R. E. *IEEE trans. on Med. Imag.* **1995**, *14*, 616.
- (42) Balazs, B.; Maxwell, R. S.; deTeresa, S.; Dihn, L. N.; Gee, R. H. *MRS Symposium Proceedings* **2002**, *731*, 3.
- (43) Gee, R. H.; Maxwell, R. S.; Dihn, L. N.; Balazs, B. “Molecular Dynamics Studies on the Effects of Water Speciation on Interfacial Structure and Dynamics in Silica-filled PDMS Composites”; MRS Symposium Proceedings, 2002.
- (44) Carr, H. Y.; Purcell, E. M. *Phys. Rev.* **1954**, *94*, 630.
- (45) Meiboom, S.; Gill, D. *Rev. Sci. Instru.* **1958**, *29*, 688.
- (46) Maxwell, R. S. *Personal Communication* **2003**.
- (47) Callaghan, P. T.; Samulski, E. T. *Macromolecules* **1997**, *30*, 113.
- (48) Gee, R. H.; Maxwell, R. S.; Balazs, B. *Polymer* **2004**, *45*, 3885.

(49) Watson, J. M.; Baron, M. G.; Zhang, G. S.; Payne, P. A. *J. Membrane Sci.* **1992**, 73, 55.

(50) Watson, J. M.; Baron, M. G. *J. Membrane Sci.* **1996**, 110, 47.

Distribution:

7	MS 0888	T. M. Alam
1	MS 0886	M. K. Alam
1	MS 0888	B. R. Cherry
1	MS 0888	R.L. Clough
1	MS 0889	Jeff Braithwaite
1		Robert Maxwell
		Lawrence Livermore National Labs (LLNL), L-029
		7000 East Ave., PO Box 800
		Livermore, CA 94551-0800
1	MS 9018	Central Technical Files, 8945-1
2	MS 0899	Technical Library, 9616
1	MS 0612	Review & Approval Desk, 9612 for DOE/OSTI